Time-Resolved Measurement of Coronal Temperature and Line-Intensity Profiles in Laser-Produced Plasmas

B. K. F. Young, R. E. Stewart, and C. J. Cerjan
University of California, Lawrence Livermore National Laboratory, Livermore, California 94550

G. Charatis and Gar. E. Busch
KMS Fusion Inc., Ann Arbor, Michigan 48104
(Received 27 June 1988)

Time-resolved electron temperature and line-intensity profiles in laser-produced plasmas have been measured for the first time with an x-ray framing camera. Temperature profiles measured from the slope of the free-bound recombination continuum in Al XIII ions are significantly lower than hydrodynamic model calculations. Simultaneous interferometric density measurements are in much closer agreement with computer simulations. Spectral-line-intensity profiles have also been measured and cannot be described by standard collisional radiative equilibrium models.

PACS numbers: 52.50.Jm, 32.30.Rj, 52.70.La

Measurements of the x-ray emission spectrum from laser-produced plasmas have been used for many years to diagnose characteristic plasma conditions such as the electron temperature and density.[1-10] In principle, the measurement of the spectral emission signature is a clean, nonperturbing way to probe the microscopic conditions existing in these hot, dense plasmas. Because of the manner in which these plasmas are created, however, they have rapid and extreme temporal variations and steep gradients that must be resolved to extract meaningful information about the plasma. We report here the results of the first measurements of the *K*-shell x-ray emission spectrum of Al XI, XII, and XIII ions in laser-produced plasmas that are simultaneously resolved in space and time. Full space-time resolution has been made possible in these experiments by our extending the techniques of microdot spectroscopy first used by Herbst *et al.*[3,4] to time-resolved measurements by the use of a gated framing crystal x-ray spectrometer (FCXS).[11] The time-resolved electron temperature profiles for a laser-produced Al plasma have been measured for the first time with the slope of the H-type free-bound recombination continuum. The electron density profiles were simultaneously measured with holographic interferometry.[12] Our techniques allow us to measure the effects of laser absorption and heat transport in the plasma corona and to clearly test standard hydrodynamic and atomic-physics-model predictions.

The experiments were conducted with the CHROMA laser facility at KMS Fusion, Inc. Simple 100-μm-diam Al microdot targets were irradiated with 10^{14} W/cm^2 of 0.53-μm light in a 1.0-ns-wide stacked pulse (a trapezoidal temporal profile with 100-ps rise and fall times and a 950-ps flat top). As the target is heated, a collisionally confined plume of Al ions is generated with a diameter approximately equal to the original dot diameter, greatly reducing the effects of transverse gradients in the plasma. This is confirmed by 2D laser interferometry measurements which indicate flat transverse density profiles for the Al dot plasma. Also, 2D LASNEX[13,14] calculations (described later in this Letter) predict flat temperature and density profiles with less than a 20% variation across the Al dot.

A wide array of diagnostics were fielded including the FCXS, a four frame holographic interferometer, a spatially resolved x-ray streaked spectrograph (XSCS), and x-ray pinhole cameras. All of these instruments were aligned to view the target edge on to within 5° of the target surface and employed a common timing fiducial. (See Fig. 1.) The FCXS provided simultaneously space- and time-resolved measurement of the x-ray emission spectra. The FCXS is based on gated microchannel plate detector[15] which has three active stripline areas which can be independently gated on and off with a fast, high-voltage bias pulse. A typical set of framed spectra from a heated Al microdot target is shown in Fig. 2. Each strip depicts the spatially resolved x-ray emission spectrum recorded at selected times during and after the laser heating pulse. The data have been corrected for taking into account the integrated reflectivity of the potassium acid phosphate (KAP) diffraction crystal,[16] filter transmission,[17] cesium-iodide-coated microchannel plate response,[18] film sensitivity,[19] and FCXS geometry.

The electron temperature profiles have been determined from the slope of the free-bound recombination continuum of H-type ions. These temperature profiles are shown in Fig. 3 (solid lines) and represent two selected 250-ps time intervals during and after the heating laser pulse. The free-bound continuum followed the usual $d[\ln I(h\nu)]/d[h\nu] = -1/kT_e$ intensity fall-off characteristic to a Maxwellian electron velocity distribution.[2] This was anticipated since the effects of hot electrons and laser-induced nonthermal electron distributions were not expected to be significant at the laser conditions used in the present work.[20]

The temperature profiles predicted by a 2D LASNEX

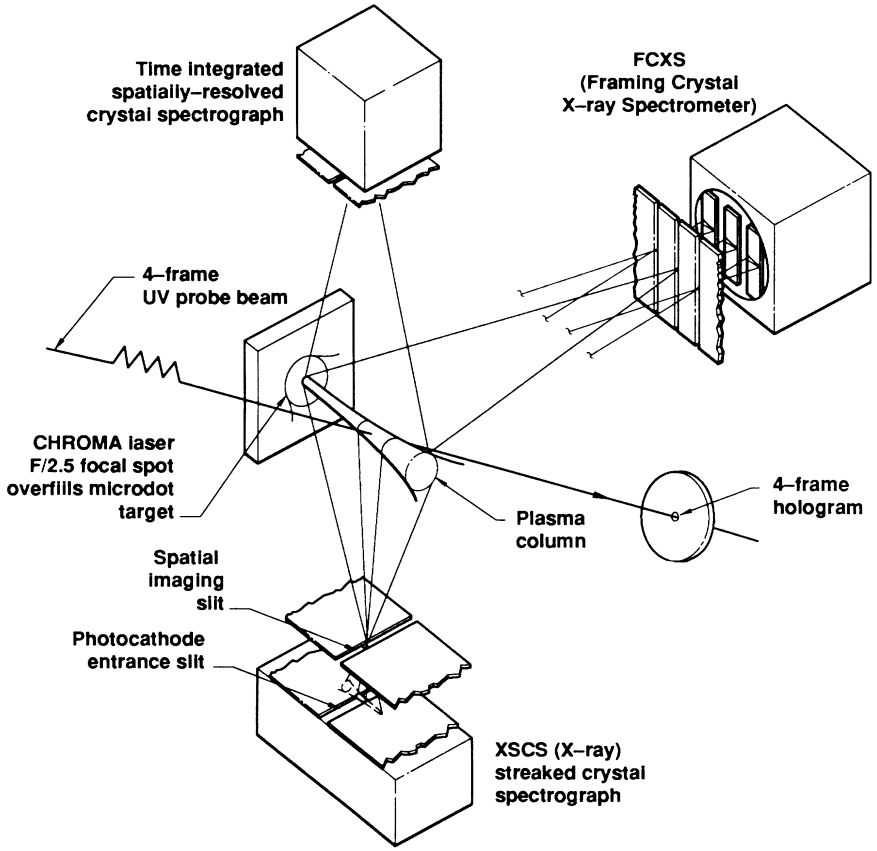

FIG. 1. The experimental setup used at the CHROMA laser facility at KMS Fusion, Inc.

hydrodynamics simulation are also shown in Fig. 3. For these calculations, we prepared a two-dimensional, cylindrically symmetric simulation assuming inverse bremsstrahlung laser light absorption, classical $T^{5/2}$ thermal conduction, and using a classical flux limiter value of 0.4. The atomic kinetics were described by a hydrogenic approximation rather than the less realistic average-atom approximation. Radiation transport was treated in the diffusion approximation, except in the x-ray regions of interest where an escape probability method was used. Temperatures representing the outer Al zones have been used for the present analysis.

The temperature profile observed while the laser is on (730–980 ps) is significantly different than the LASNEX calculated profiles. The measured temperatures are a factor of 3 lower near the target surface and continually rise for at least 200 μm, while the predicted temperatures peak at 50 μm and monotonically decrease from 100 μm outward in the simulation. Systematic experimental uncertainties in the laser intensity profile or a slight misalignment of the microdot target cannot account for the large observed differences. We note that indications of anomalously low temperatures have also been seen at these laser intensities using Raman scattering.[21] For later times, the observed temperature profiles are in better agreement with the simulation, although slightly higher and with larger spatial gradients than predicted. The observed late-time temperature profiles seem to be correlated with the variations seen in the H-type and He-type resonance line intensities. The elec-

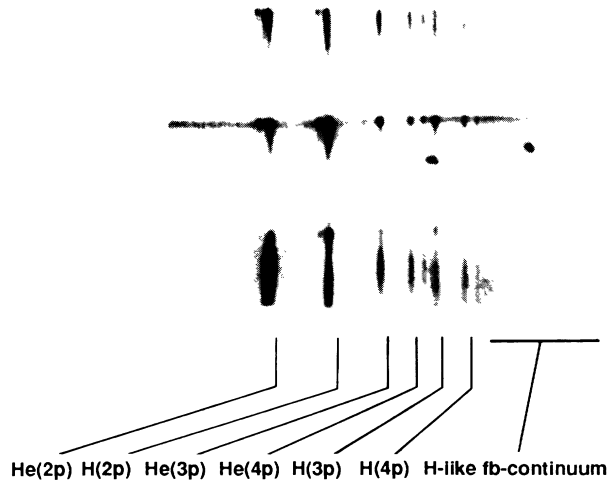

FIG. 2. A typical framed spectra measured with the FCXS. The time intervals are 1230–1480 ps (top image), 730–980 ps (center), and 1730–1980 ps (bottom) relative to the beginning of the laser heating pulse.

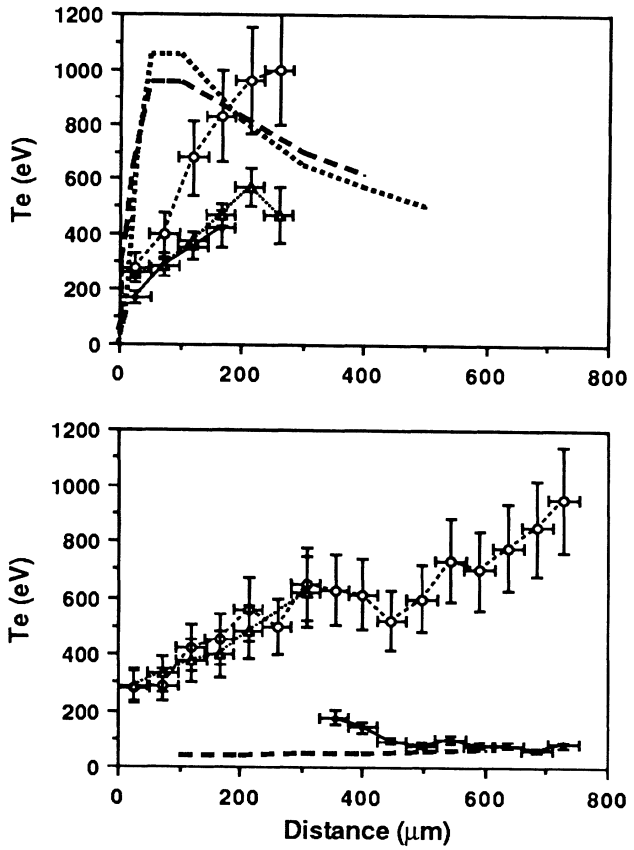

FIG. 3. Electron temperature profiles at various times during and after the laser heating pulse are presented: 730–980 ps (top) and 1950–2200 ps (bottom). LASNEX hydrodynamic code simulations [dashed lines are for 730 ps (top) and 1950 ps (bottom); dotted line is at 950 ps] are compared to experimental temperature profiles determined from the slope of the H-type free-bound continuum (solid dots), and using a steady state CRE $Ly_\beta/(^1D_2)$ satellite line ratio (triangles) and the He_β/Ly_β resonance line ratio (open dots).

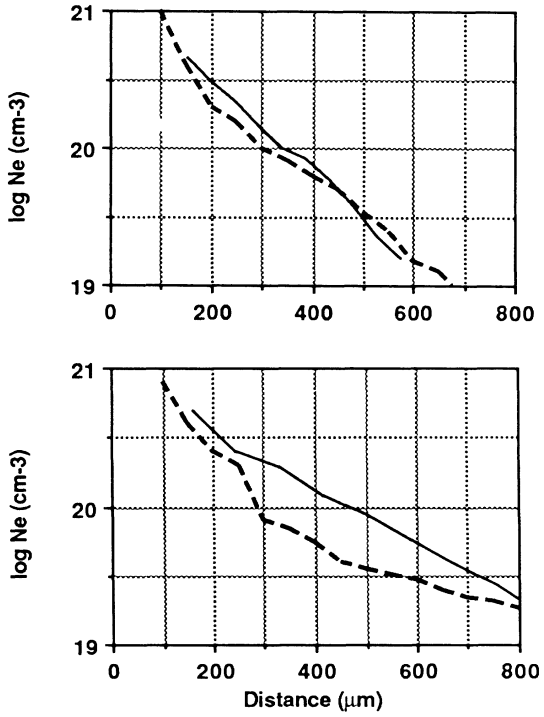

FIG. 4. The electron (axial) density profiles predicted by the LASNEX hydrodynamic code simulations (dashed lines) are compared to laser interferometry density profiles (solid lines) at 857 ps (top) and 1657 ps (bottom).

tron density profiles predicted by the LASNEX simulation are generally in good agreement with measurements with holographic interferometry at 857 and 1657 ps, and are shown in Fig. 4. An overly rapid expansion in the simulation, transverse to the laser axis, could account for the lower electron densities and temperatures seen in the model at late times and large distances from the target surface. These new data indicate that for these simple laser-plasma interaction experiments, the absorption or transport mechanisms and possibly atomic processes are not adequately understood. Further experiments of this type should help resolve these discrepancies.

The electron temperatures were also deduced with standard line-ratio diagnostics including the H-type $1s$-$3p$ resonance to He-type $1s2p(^1P_1)$-$2p^2(^1D_2)$ dielectronic satellite line ratio (triangles). (See Fig. 3.) These temperatures were determined by our comparing experimental to theoretical line ratios calculated with a collisional radiative equilibrium (CRE) modeling code RATION,[22] which is based on a steady-state ionization distribution. Optical trapping effects were included in the CRE model with a simple escape-factor correction. Although the use of a stationary model may be regarded as inappropriate, this represents an often used method for diagnosing these laser-produced plasmas. The dielectronic satellites to the Ly_α and He_α resonance lines are observed during and after the laser pulse, and exhibit a sharp intensity gradient away from the target surface, as seen in previous experiments. During the heating laser pulse, the satellite line-ratio temperature profile closely agrees with the temperatures measured from the recombination continuum. The dielectronic satellite line ratios are in good agreement with theory despite the overionization seen in the spectra due to both lines originating primarily from the H-type ground state in a thermal plasma, making this ratio relatively insensitive to the ionization distribution. After the laser pulse, the plasma is recombining. The resonance lines are significantly populated by recombination processes and the CRE analysis clearly fails.

We have also used the He-type $1s^2(^1S_0)$-$1s3p(^1P_1)$ to H-type $1s$-$3p$ "He_β/Ly_β" resonance line ratio (open dots) to determine the CRE ionization temperature both during and after the laser pulse. (See Fig. 3.) The He_β/Ly_β resonance line-ratio temperatures are much

higher and indicate that the plasma is overionized with respect to a CRE plasma. It is interesting to note that during the laser pulse, both CRE line-ratio temperature profiles show the same qualitative deviation from the LASNEX model prediction. Also, most of the line emission observed at distances greater than 100 μm from the target surface is emitted after the laser pulse. Thus previous spatially resolved, time-integrated spectroscopic measurements of coronal temperature and density profiles may be in error. The ionization distribution must be independently determined to compensate for the lack of ionization equilibrium in these nonstationary plasmas. A number of such nonstationary modeling schemes are presently being investigated.[5,9,10]

In conclusion, simultaneously space- and time-resolved Al K-shell x-ray spectra have been measured from laser-irradiated microdot targets. Space- and time-resolved electron temperature and density profiles have been independently determined. During the heating laser pulse, the spectral features that are most sensitive to the electron velocity distribution function, the free-bound continuum and the He-type dielectronic satellite to the Ly_β line ratio, give consistent temperatures. These measurements of the electron temperature profile, resolved for the first time, are significantly different than 2D LASNEX hydrodynamic simulations. Even the He_β/Ly_β resonance line-intensity ratio temperature profiles (based on a CRE analysis) disagree qualitatively with hydrodynamic calculations. Further work is needed to resolve these differences. The highly transient ionization distribution of this laser plasma complicates the population kinetics required to fully describe the emission spectra and warrants further examination. This work demonstrates that simultaneously space- and time-resolved diagnostics minimize the effects of unresolved gradients in x-ray spectroscopy data, and are essential for the study of laser absorption, heat transport, and atomic physics of laser-produced plasmas.

The authors gratefully acknowledge the efforts of the excellent staff at KMS Fusion and the very helpful discussions with D. Bailey, R. Cauble, W. Goldstein, and R. Walling of LLNL. We would especially like to thank M. Rosen of LLNL for his fruitful discussions and suggestions. This work was performed jointly under the auspices of the U.S. Department of Energy by Lawrence Livermore National Laboratory under Contract No. W-7405-Eng-48 and by KMS Fusion, Inc. under Contract No. DE-AC08-82-DP40152.

[1]J. P. Apruzese, D. Duston, and J. Davis, J. Quant. Spectrosc. Radiat. Transfer **36**, 339 (1986).

[2]C. DeMichelis and M. Mattioli, Nucl. Fusion **21**, 677 (1981).

[3]M. J. Herbst *et al.*, Rev. Sci. Instrum. **53**, 1418 (1982).

[4]P. G. Burkhalter *et al.*, Phys. Fluids **26**, 3850 (1983).

[5]V. A. Boiko, I. Yu. Skobelev, and A. Ya. Faenov, Fiz. Plazmy **10**, 143 (1984) [Sov. J. Plasma Phys. **10**, 82 (1984)].

[6]J. -C. Gauthier *et al.*, J. Phys. D **16**, 1929 (1983).

[7]Ph. Alaterre *et al.*, Opt. Commun. **49**, 140 (1984).

[8]M. H. Key *et al*, Phys. Rev. Lett. **44**, 1669 (1980).

[9]R. L. Kauffman, R. W. Lee, and K. Estabrook, Phys. Rev. A **35**, 4286 (1987).

[10]R. W. Lee, J. Quant. Spectrosc. Radiat. Transfer **27**, 87 (1982).

[11]B. K. F. Young, G. Charatis, Gar. E. Busch, and R. E. Stewart, to be published.

[12]Gar. E. Busch, C. L. Shepard, L. D. Siebert, and J. A. Tarvin, Rev. Sci. Instrum. **56**, 879 (1985).

[13]G. B. Zimmerman and W. L. Kruer, Comments Plasma Phys. Controlled Fusion **2**, 51 (1975).

[14]M. D. Rosen and D. S. Bailey, private communication.

[15]B. K. F. Young, R. W. Stewart, J. Bailey, and J. G. Woodworth, Rev. Sci. Instrum. **57**, 2729 (1986).

[16]A. Burek, Space Sci. Instrum. **2**, 53 (1976).

[17]B. L. Henke *et al.* At. Data Nucl. Data Tables **27**, 1 (1982).

[18]G. W. Fraser *et al*, Nucl. Instrum. Methods Phys. Res. **224**, 272 (1984).

[19]Each piece of film was preexposed to a calibrated optical step wedge determining the film sensitivity for each target shot.

[20]C. E. Max, in *Laser-Plasma Interaction,* Proceedings of the Les Houches Summer School of Theoretical Physics, Session XXXIV, edited by R. Balian and J. C. Adam (North-Holland, Amsterdam, 1981), p. 301.

[21]R. P. Drake *et al*, Phys. Fluids **31**, 1795 (1988). (Note: Drake measures similar 400–500-eV coronal temperatures during the heating laser pulse at $n_e \approx 10^{21}$ cm^{-3}.)

[22]R. W. Lee, B. L. Whitten, and R. E. Strout, II, J. Quant. Spectrosc. Radiat. Transfer **32**, 91 (1983).

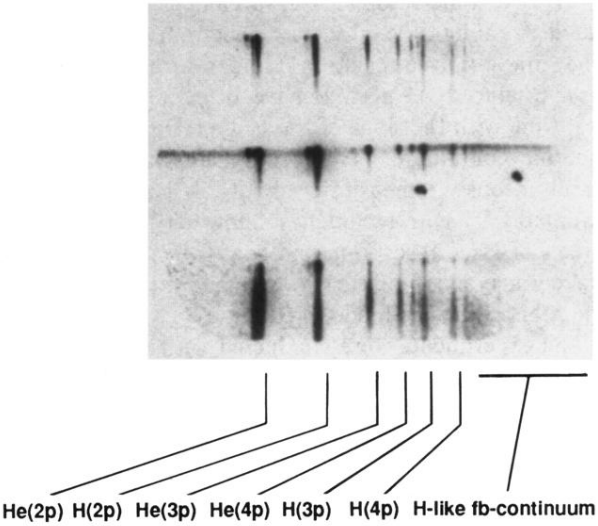

FIG. 2. A typical framed spectra measured with the FCXS. The time intervals are 1230–1480 ps (top image), 730–980 ps (center), and 1730–1980 ps (bottom) relative to the beginning of the laser heating pulse.